Intercalation of *n*-Alkylamines in $FePS_3$

Pattayil Alias Joy and Sukumaran Vasudevan*

Department of Inorganic and Physical Chemistry, Indian Institute of Science, Bangalore 560 012, India

Received January 5, 1993. Revised Manuscript Received May 27, 1993

The intercalation of linear alkylamines (C_1-C_4) in the two-dimensional (2D) Ising antiferromagnet, $FePS_3$, has been investigated. Intercalation proceeds with a dilation of the interlayer distance. The expansion (~3.8 Å) is the same for all four amine molecules, suggesting that they are oriented flat with respect to the layers. From an analysis of the products of deintercalation, it is concluded that the intercalated species are the alkylammonium cations and neutral amine molecules. The intercalated compounds are highly moisture sensitive, as reflected in the chemical nature of the intercalated species. Charge neutrality of the lattice after intercalation is preserved by the loss of Fe^{2+} ions from the lattice. These Fe^{2+} ions are further oxidized to form superparamagnetic Fe_2O_3 clusters, as confirmed by Mössbauer spectra and magnetic measurements. This was further corroborated by *in situ* EPR studies. The ^{57}Fe Mössbauer spectra of the intercalated compounds showed evidence for two species other than Fe_2O_3. On the basis of the observed isomer shifts and quadrupole splittings, they have been assigned to Fe^{2+} in an environment similar to that in $FePS_3$ and in a distorted $FePS_3$ environment. The temperature and field dependence of the magnetic susceptibility of single crystals of the amine-intercalated $FePS_3$ have been measured. Their magnetic behavior shows many of the features expected of a 2D Ising antiferromagnet with random defects, $Fe_{1-x}PS_3$, in agreement with the mechanism of intercalation.

Introduction

The intercalation chemistry of the transition-metal thiophosphates provides one of the most intriguing and fascinating facets of the intercalation phenomena. What was once considered as a straightforward extension of the ideas and charge-transfer models developed for the intercalation reaction of the transition-metal dichalcogenides now turns out to be much richer and more complex. The transition-metal thiophosphates, MPS_3 (M = Mn, Fe, Co, etc.),[1] are a class of insulating layered compounds structurally similar to the early transition-metal dichalcogenides, MX_2 (M = Ti, Nb, Ta and X = S, Se)[2] and, like the latter, can intercalate a wide variety of electron-donating molecules within their van der Waals gap.[3,4] Their structure may be derived from the MX_2 structure by replacing every third metal atom with a P_2 pair. The nature of metal-ligand interactions in these two classes of compounds is, however, quite different. The transition-metal thiophosphates are much more ionic. Their optical,[5] electrical, and magnetic properties[6] are best explained using crystal-field theory rather than the covalent band model as in the case of MX_2 compounds.[2]

An important feature of the transition-metal thiophosphates, different from most other layered compounds, is that they are magnetic, with the divalent M^{2+} ion in the high-spin state.[7] MPS_3 (M = Mn, Fe, and Ni) order antiferromagnetically at low temperatures. An interesting feature of the magnetism in MPS_3 is that the anisotropy of the magnetic exchange interaction $\mathbf{H}_{ex} = -2\sum[J_{xy}(S_{ix}S_{jx} + S_{iy}S_{jy}) + J_zS_{iz}S_{jz}]$, is strongly dependent on the metal ion.[6] The anisotropy originates from crystal field effects as a consequence of the zero field splitting of the M^{2+} ion d levels due to the trigonal distortion of the MS_6 octahedra. The magnetic susceptibility of $FePS_3$ is highly anisotropic and the magnetic behavior is best described as a 2D Ising antiferromagnet, $\mathbf{H}_{ex} = -2\sum J_zS_{iz}S_{jz}$, $J_{xy} = 0$. In contrast, the magnetic behavior of $MnPS_3$ is isotropic while $NiPS_3$ shows weak anisotropy with $J_{xy} > J_z$ in $\mathbf{H}_{ex}$.

Intercalation in $NiPS_3$ and $FePS_3$ has attracted attention. These have been considered as potential cathode materials since, like TiS_2,[8] they can reversibly intercalate lithium.[3,9] The chemistry of the process is, however, quite different. On the basis of ^{57}Fe Mössbauer[10,11] and Ni K-edge EXAFS,[12] it has been suggested that in Li_xFePS_3 and Li_xNiPS_3 part of the divalent transition metal is reduced to the zero oxidation state and that these species form diamagnetic domains. In the case of Li_xNiPS_3 it has been claimed that the Ni(0) moves to tetrahedral sites of the lattice. There are a number of open questions—the mechanism of the two-electron transfer and the absence of any change in structure or magnetic behavior observed on intercalation.

In this paper we describe the use of Mössbauer spectroscopy, EPR, single-crystal magnetic susceptibility, and

(1) Klingen, W.; Ott, R.; Hahn, H. *Z. Anorg. Allg. Chem.* **1973**, *396*, 271.
(2) Wilson, J. A.; Yoffe, A. D. *Adv. Phys.* **1969**, *73*, 193.
(3) Brec, R. *Solid State Ionics* **1986**, *22*, 3.
(4) Johnson, J. W. In *Intercalation Chemistry*; Whittingham, M. S., Jacobson, A. J., Eds.; Academic: New York, 1982.
(5) Joy, P. A.; Vasudevan, S. *Phys. Rev.* **1992**, *B46*, 5134.
(6) Joy, P. A.; Vasudevan, S. *Phys. Rev.* **1992**, *B46*, 5425.
(7) Le Flem, G.; Brec, R.; Ouvrard, G.; Louisy, A.; Segransan, P. *J. Phys. Chem. Solids* **1982**, *43*, 455.
(8) Whittingham, M. S. *Prog. Solid State Chem.* **1978**, *12*, 41.
(9) Thompson, A. H.; Whittingham, M. S. *Mater. Res. Bull.* **1977**, *12*, 741. Le Mehaute, A.; Ouvrard, G.; Brec, R.; Rouxel, J. *Mater. Res. Bull.* **1977**, *12*, 1191.
(10) Fatseas, G. A.; Evain, M.; Ouvrard, G.; Brec, R.; Whangbo, M.-H. *Phys. Rev.* **1987**, *B35*, 3082.
(11) Colombet, P.; Ouvrard, G.; Antson, O.; Brec, R. *J. Magn. Magn. Mater.* **1987**, *71*, 100.
(12) Ouvrard, G.; Prouzet, E.; Brec, R.; Benazeth, S.; Dexpert, H. *J. Solid State Chem.* **1990**, *86*, 238.

0897-4756/93/2805-1182$04.00/0

temperature-programmed deintercalation to investigate the intercalation of linear aliphatic amines (C_1–C_4) in $FePS_3$. The objective is to understand the mechanism of and changes occurring on intercalation, i.e., to see whether these are similar to the behavior of lithium intercalation or are different, as in the case of pyridine intercalation in $MnPS_3$.[13] In this case direct spectroscopic evidence had been presented to prove that the intercalated species are pyridinium ions solvated by neutral pyridine molecules, with charge neutrality being preserved by the loss of Mn^{2+} ions from the lattice. The mechanism is similar to the ion-exchange intercalation first described by Clement et al.[14] for the intercalation of organometallic cations in the transition-metal thiophosphates.

Intercalation of amines in $FePS_3$ was found to proceed by the ion-exchange mechanism. The intercalated species appear to be solvated alkylammonium cations. Charge neutrality is preserved by the loss of Fe^{2+} ions from the lattice. It is shown that the magnetic properties of the intercalated $FePS_3$ has many of the attributes of a 2D antiferromagnetic Ising lattice with defects. The situation is complicated by the fact that the Fe^{2+} ions removed from the lattice are further oxidized to Fe^{3+}. We have thus been forced to use a combination of techniques to understand the true intercalation chemistry in these compounds.

Experimental Section

$FePS_3$ powders and single crystals were prepared from the corresponding elements following procedures reported in the literature.[1,15] $FePS_3$ powders are not stoichiometric; their EPR spectra show a signal characteristic of Fe^{3+}. This feature has been observed and reported by a number of workers.[11] The concentration of Fe^{3+} is, however, low, and is not seen in the Mössbauer spectrum. A gravimetric estimation of the iron content in $FePS_3$ showed that within the accuracy (±3%) of the technique the compound is stoichiometric.

Methylamine and ethylamine were generated by dropping their aqueous solutions (S. D. Fine Chemicals) over KOH pellets. The amines so generated were dried by passing through a KOH tower and condensed in a liquid nitrogen trap. They were further purified by distilling under vacuum using a series of liquid nitrogen traps. (The amines so obtained are still not completely anhydrous as seen in their mass spectra which showed traces of H_2O, m/e = 18.) Propyl- and butylamines (Riedel-De Hahn) were dried in a similar manner. The amines were condensed over $FePS_3$ powder taken in glass ampules and sealed under vacuum. Intercalation of $FePS_3$ by direct contact with methyl- and ethylamine liquid was extremely rapid even at room temperature. The complete reaction took place within 60 min. Intercalation proceeded with considerable swelling of the powders and breaking up of the crystals. To maintain the integrity of the crystals, intercalation was consequently effected by equilibration of the host crystals with amine vapor at room temperature. Complete intercalation through this procedure took over 2 weeks. The supernatant amine liquid remained colorless, implying that there is no loss of sulfur from the host compounds (sulfur in amines has an intense reddish color). Analysis of the supernatant amine liquid after complete intercalation showed no trace of Fe^{2+} ions.

On exposure to air, the intercalated samples slowly changed their color from black to dark brown. The change in color was most rapid in methylamine-intercalated compounds and slowest in the butylamine-intercalated compounds. Consequently, extreme care was taken to avoid exposure of the samples to atmosphere.

The extent of intercalation was verified by powder XRD (Philips PW1050; Cu Kα, λ = 1.542 Å). Absence of the 00l reflections of the host, $FePS_3$, was considered as evidence for complete intercalation. Stoichiometry was established by TGA (Ulvac Sinku-Rico TA1500) in a flow of dry oxygen-free N_2.

The chemical identity of the intercalated species was probed using temperature-programmed deintercalation spectroscopy (TPDS). This technique is identical to the thermal desorption spectroscopy (TDS).[16] The intercalated samples were heated at a linear rate, and the volatile deintercalating molecules analyzed by a mass spectrometer.

The output of the experiment is a temperature profile for each deintercalating mass (counts vs temperature for each deintercalating m/e). The sum of the counts for each m/e vs temperature, i.e., the total ion counts (TIC) vs temperature gives information complementary to a TG run. In a TG run, the weight loss is recorded as a function of temperature, whereas in TPDS, the amount of gaseous products evolving as a function of temperature is monitored. The main advantage of TPDS is that the gas evolved can be analyzed for different masses, so that the composition of different products as a function of temperature can be monitored. The temperature at which the rate of appearance of a gaseous species is at the maximum is a measure of the activation barrier for deintercalation or for the formation of the species within the layer. The appearance of more than one peak in the temperature profile is indicative of intercalated species with different strengths of interaction or different rates of reaction/formation.

TPDS studies were done in a modified GC-MSD system, HP 5890-5970. In a TPDS experiment, the intercalated samples were heated at a constant heating rate, 10 K/min (300–675 K), in a stream of helium. The volatile deintercalating products in the mass range m/e = 10–400 were analyzed online using a quadrupole mass spectrometer. The data were collected on an HP 9000, 200 series computer. In a typical TPDS run, the intercalated material was placed in a thin-walled stainless steel tube. The tube occupied the same position as the column in the GC and was connected to the MS by a silicone capillary. The other end of the tube was connected to a He cylinder. The temperature of the oven was controlled to ±1 K by the control circuit provided in the GC, which also provided variable linear rates of heating.

Electrical conductivities between 77 and 300 K were measured on pressed pellets of the powder samples by an ac two-probe technique using a Wayneker B642 autobalance universal bridge operating at 1591.8 Hz ($\omega = 10^4$ Hz).

The magnetic susceptibility was measured on crystals in the 55–375 K temperature range using a vibrating sample magnetometer (VSM) EG&G PAR 155. Crystals of the sample were attached to the end of a wedge-shaped Teflon piece. The magnetometer was calibrated using $Hg[Co(NCS)_4]$ as the standard. In magnetic susceptibility measurements, $\chi_{\parallel}$ is defined as the susceptibility with the external magnetic field perpendicular to the ab plane (the layer). The definition is the same for both pure and intercalated $FePS_3$.

EPR spectra were recorded on an X-band Varian E109 E-line century series EPR spectrometer.

Mössbauer spectra of the powder samples were recorded on a homemade constant-acceleration spectrometer with a ^{57}Co source in Pd matrix (5 mCi). Data were collected using a microprocessor-controlled multichannel analyzer (512 channels) and later transferred to a computer for further analysis. The velocity scale was calibrated with the six finger pattern obtained from an iron foil at room temperature.

Mössbauer spectra were deconvoluted as a sum of Lorentzians and fitted by the least-squares method. The parameters used in the fitting procedure are intensity, position, width, and the quadrupole splitting of the observed doublets, as well as the total number of doublets. On output, the program gave the normalized spectra (counts vs velocity in mm/s) as a sum of the Lorentzians, and the isomer shifts of each species with respect to iron.

For most of the amine-intercalated samples, vibrational and optical spectra could not be recorded because of the high absorbance of the samples. The IR spectra in the 100–700-cm^{-1}

(13) Joy, P. A.; Vasudevan, S. *J. Am. Chem. Soc.* **1992**, *114*, 7792.
(14) Michalowicz, A.; Clement, R. *Inorg. Chem.* **1982**, *21*, 3872.
(15) Nitsche, R.; Wild, P. *Mater. Res. Bull.* **1970**, *5*, 419. Taylor, B. E.; Steger, J.; Wold, A. *J. Solid State Chem.* **1973**, *7*, 461.
(16) Cvetanovic, R. J.; Amenomiya, Y. *Catal. Rev.* **1972**, *6*, 21.

Table I. Basal Spacings from Powder XRD Data

compound	d (Å)	Δd (Å)
$FePS_3$	6.394	
$FePS_3$–CH_3NH_2	10.165	3.771
$FePS_3$–$C_2H_5NH_2$	10.222	3.828
$FePS_3$–$C_3H_7NH_2$	10.281	3.888
$FePS_3$–$C_4H_9NH_2$	10.357	3.963

region could be recorded, but the resolution and the overall signal-to-noise ratio were poor. Since the intercalated crystals were extremely fragile, it was not possible to cleave them as was done for recording the spectra of the pure host crystals. Far-infrared spectra (700–100 cm^{-1}) were recorded on a Bruker IFS 113-V FTIR spectrometer on pressed polyethylene pellets. The IR spectra of the intercalated compounds in the 700–100-cm^{-1} region were similar to those of the pure host.

Results and Discussion

Structure. The XRD patterns of the amine-intercalated powder samples were of poor quality and showed only a few broad lines. The broadening is due to the small size of the crystallites, probably because of the extreme reactivity of the amines with $FePS_3$. For methyl- and ethylamine intercalated samples prepared by the direct contact of the amine liquid with $FePS_3$ powder, the crystallite size as estimated using the Scherrer equation[17] for the broadening of the X-ray profile, is ~150 Å. Even in situations where the crystal integrity was preserved after intercalation, Weisenberg photographs showed spots only for the 00l reflections while all other reflections appeared as streaks. This suggests considerable mosaic in the structure. The host 00l lines were completely absent in the powder XRD, thus providing evidence for complete intercalation. New 00l reflections were observed corresponding to a lattice expansion along the c axis. In most samples only 00l type reflections were observed. The lattice expansions of the various amine intercalates are summarized in Table I. The fact that lattice expansion changes only marginally in going from methylamine to butylamine, implies that the molecules have essentially a flat orientation with respect to the layers. The observed expansion is comparable to the van der Waals diameter of the methyl group[18] (3.6 Å). The slight increase in Δd, in going from methylamine to butylamine, is similar to that observed in TaS_2 probably because the amines are not exactly flat but at a slight angle with respect to the layers.[19] Since non-00l reflections were too weak to be observed, the determination of lattice parameters (other than c) was not possible.

The TGA thermograms of the amine-intercalated compounds showed a fairly complex pattern. Most compounds showed a three-step weight loss (Figure 1), but the relative magnitude of the three steps differed from sample to sample, even for the same amine. For a particular amine, however, the temperatures of the three steps were reproducible. For the heavier amines, the three steps were not so clearly delineated and a continuous weight loss was observed right up to the decomposition temperature of the host lattice.

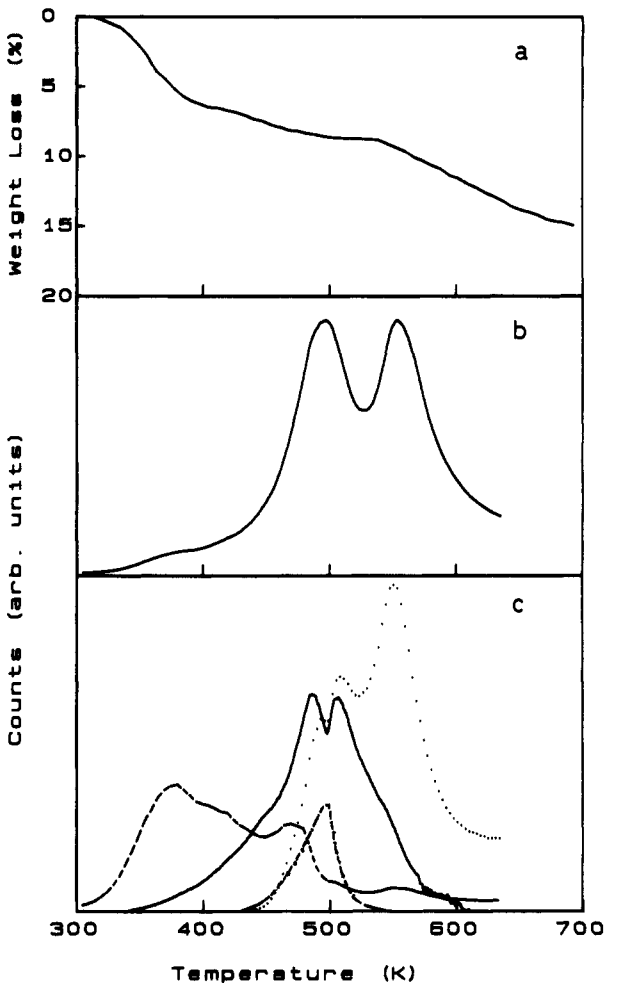

Figure 1. TG and TPDS of methylamine-intercalated $FePS_3$. (a) TG, (b) total ion count (TIC) as a function of temperature, and (c) TPD profile for CH_3NH_2, m/e = 31 (—), H_2O, m/e = 18 (– – –); H_2S, m/e = 34 (· · ·); S, m/e = 64 (– · –).

It was not possible to estimate the amine stoichiometries from TGA. There appeared to be a partial decomposition of the host lattice at a fairly low temperature, 550 K, which was later confirmed by temperature-programmed deintercalation (TPDS). Pure $FePS_3$ decomposes above 773 K. As may be seen in Figure 1a, the weight losses in the TGA do not show sharp steps, so that it was not possible to clearly define where amine deintercalation stops and where lattice decomposition starts. An additional complication was that the total as well as the relative magnitude of the steps showed a strong dependence on the extent of drying of the amines prior to intercalation and even a brief exposure to the atmosphere changed the TGA profile, enhancing the first weight loss. The latter was unavoidable during the transfer of the intercalated material to the TGA apparatus. A similar effect had been observed for pyridine-intercalated $MnPS_3$ and has been ascribed to the exchange of neutral intercalated pyridine molecules with H_2O molecules from the atmosphere.[13] The effect, however, is much more pronounced in the amine-intercalated $FePS_3$. One may, however, calculate an upper limit for the amine stoichiometry from the TGA. These are ($FePS_3$:amine) 1:1 for methyl- and ethylamines and 1:0.8 for propyl- and butylamines. These values, surprisingly, are similar to

(17) Klug, H. P.; Alexander, L. E. *X-Ray Diffraction Procedures*; John Wiley & Sons: New York, 1974.

(18) Pauling (Pauling, L. *The Nature of the Chemical Bond*; Oxford & IBH: Calcutta, 1963; p 261) gives the van der Waals diameter of the methyl group as 4.0 Å, but more recent crystallographic data (Dunitz, J. P. *X-Ray Analysis and the Structure of Organic Molecules*; Cornell University Press: Ithaca, NY, 1979; p 110.) suggests that the excluded volume of the methyl group is 23.5 $Å^3$ and that of the NH_2 group is 19.0 $Å^3$. The corresponding diameters of these groups would be 3.55 and 3.31 Å, respectively.

(19) Gamble, F. R.; Osiecki, J. H.; Cais, M.; Pisharody, R.; DiSalvo, F. J.; Geballe, T. H. *Science* **1971**, *174*, 493.

the stoichiometries reported by Foot et al. for amine intercalation in $NiPS_3$.[20]

TPD Spectra. The output of the experiment is a temperature profile for each deintercalating mass. The appearance of more than one peak in the temperature profile is indicative of intercalated species with different strengths of interaction. The TPD of $FePS_3(CH_3NH_2)$ is shown in Figure 1. Figure 1b is the total ion concentration as a function of temperature. It shows three broad peaks at 380, 496, and 553 K. These temperatures are similar to the temperatures at which weight losses are observed in the TG. The spectral analysis of Figure 1 is more interesting. Figure 1c shows the temperature profiles for CH_3NH_2 m/e = 31, H_2O m/e = 18, H_2S m/e = 34, and S m/e = 64. In addition, masses corresponding to phosphorus sulfides (P_2S m/e = 95, P_2S_3 m/e = 158 etc.) were also observed. Their deintercalation profiles were not complete until 673 K and are not shown in the figure. The amine profile shows a broad band at 435 K and two sharp features at 487 and 506 K while the H_2S profile shows features at 493 and 510 K as well as at high temperature, 553 K. The H_2O profile shows a broad peak at 375 K, suggestive of a physisorbed species, as well as a peak at ~487 K. The amine profile is evidence for more than one type of amine in the intercalated species.

The two major features are (i) a rather complicated amine profile and (ii) the large amount of H_2S and sulfur as well as phosphorus sulfides. The presence of the latter implies a breaking up of the host lattice on thermal deintercalation.

In interpreting the TPD profile of amine we have extended the model proposed for the TPD of pyridine from intercalated $MnPS_3$.[13] As mentioned in the Introduction, pyridine is intercalated as pyridinium ions solvated by neutral pyridine molecules with charge neutrality being preserved by loss of Mn^{2+} from the lattice to give $Mn_{1-x}PS_3(pyrH^+)_{2x}(pyr)_y$. On deintercalation the pyridinium ions combined with lattice sulfur to give neutral pyridine and H_2S. There is also a partial breaking up of the lattice. Consequently it is assumed that in $FePS_3$-(amine) also the intercalated species are alkylammonium cations solvated by the neutral amine. This assumption is not very drastic since in the case of methylamine intercalation in $NiPS_3$, Foot et al. have found evidence for the presence of the methylammonium cations.[20]

The broad methylamine feature at 435 K in the amine spectra is assigned to the deintercalation of neutral amine, since no other species have features at this temperature. The fact that the two sharp amine features are associated with the liberation of H_2S suggests that originally they were present in the cationic form and that on raising the temperature, amine and H_2S are formed by the reaction schemes

$$2RNH_3^+ + S^{2-}(\text{lattice}) \rightarrow 2RNH_2 + H_2S$$

$$RNH_3^+ + H_2O \rightleftharpoons RNH_2 + H_3O^+$$

$$2H_3O^+ + S^{2-}(\text{lattice}) \rightarrow 2H_2O + H_2S$$

The presence of phosphorus sulfides in the deintercalation profile implies a partial breaking up of the $FePS_3$ lattice. Thus, TPDS provides indirect evidence for a protonated amine (RNH_3^+) in the amine intercalated $FePS_3$. The source of protons is likely to be H_2O molecules which are always associated with the amines. The protonated amines are likely to be solvated by neutral amines, $(RNH_3^+)_{2x}(RNH_2)_y$. Similar TPD profiles are also observed for ethylamine in $FePS_3$. The case of propyl and butylamine samples is more complicated because of the possibility of a number of side reactions, some of which may have taken place in the gas phase.

As in the case of the TGA experiments, just a brief exposure of the intercalated samples to the atmosphere changed their TPD profiles. The H_2O profile now shows a pronounced peak at 393 K. The amine profile shifts to lower temperatures with a sharp shoulder at 400 K. This implies a strong association between amine and water molecules in the intercalated state. A probable explanation is an exchange between the physisorbed water (373 K) and neutral amine molecules.

To summarize, TPD spectra of the amine-intercalated compounds agree with the TGA results and show (i) the presence of more than one type of amine species—there is indirect evidence that one of the species is the protonated amine, RNH_3^+, and the other netural amine, and (ii) thermal deintercalation proceeding with a breaking up of the host lattice at temperatures lower than the decomposition temperature of the host.

Electrical Properties. The amine-intercalated $FePS_3$ compounds are insulators. Their room-temperature resistivities being of the order of 10^5 Ω cm, comparable to that of $FePS_3$. The activation energy for $FePS_3$-methylamine as obtained from log ρ vs $1/T$ plot is 1.7 eV. For $FePS_3$ the reported bandgap from optical measurements is 1.6 eV.[21] The resistivities of the other amine intercalates are identical.

The insulating nature of the intercalated compounds suggests that if at all charge transfer has taken place, it must be to localized states of $FePS_3$. It has been reported that on intercalation of lithium in $FePS_3$, fairly substantial changes in conductivity occur (no stoichiometries or temperature variation was reported).[22] If true, this implies that amine intercalation in $FePS_3$ proceeds by a mechanism different from that of lithium intercalation. In contrast, in the transition-metal dichalcogenides, both lithium and amine intercalations are accompanied by changes in conductivity.[23] Both proceed by a charge-transfer mechanism in which the host lattice acceptor states are identical.

Mössbauer Spectra. To identify the states involved in the intercalation process, the room temperature Mössbauer spectra of the amine-intercalated $FePS_3$ were recorded. Typical Mössbauer spectra of the amine-intercalated $FePS_3$ are shown in Figure 2. It is interesting to note that in all the amine compounds (C_1–C_4), the quadrupolar doublet due to Fe^{2+} in an $FePS_3$ like environment is obtained, but with varying intensities. The Mössbauer spectra of all four amine-intercalated compounds showed additional features. These are most prominent and resolved in the methylamine-intercalated compound. It may be seen that with increasing chain length of the amines the contribution of these additional features to the overall spectra appears to decrease. Thus

(20) Foot, P. J. S.; Shaker, N. G. *Mater. Res. Bull.* **1976**, *18*, 173.

(21) Aruchamy, A.; Berger, H.; Levy, F. *J. Solid State Chem.* **1988**, *72*, 316.

(22) Brec, R.; Schleich, D. M.; Ouvrard, G.; Louisy, A.; Rouxel, J. *Inorg. Chem.* **1979**, *18*, 1814.

(23) Friend, R. H.; Yoffe, A. D. *Adv. Phys.* **1987**, *36*, 1.

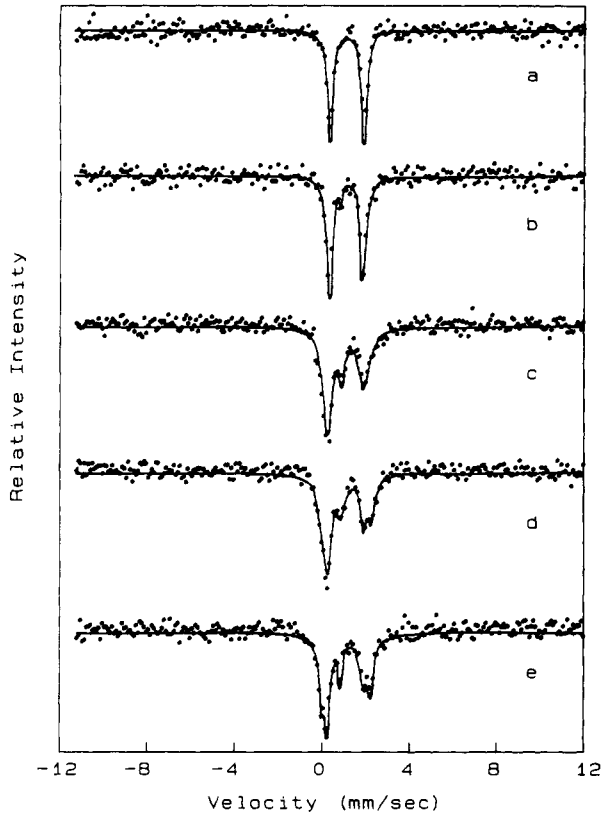

Figure 2. Mössbauer spectra of $FePS_3$ and amine-intercalated $FePS_3$ samples. Circles are experimental points, and solid lines represent the least-squares fitted curves: (a) $FePS_3$; (b) $FePS_3$–$C_4H_9NH_2$; (c) $FePS_3$–$C_3H_7NH_2$; (d) $FePS_3$–$C_2H_5NH_2$; (e) $FePS_3$–CH_3NH_2.

in the butylamine-intercalated sample only a broadening of the original doublet is seen. The feature at 0.78 mm/s is seen in all the samples.

The observed spectra of all four amine compounds could be fitted with three doublets. The fitted parameters viz., isomer shifts and quadrupole splitting, are given in Table II. The three doublets (features A, B, and C) are shown in dotted lines in Figure 3 for methylamine- and butylamine-intercalated $FePS_3$. Typical linewidths (fwhm) for A, B, and C for the butylamine-intercalated compound are 0.28, 0.46, and 0.26 mm/s, respectively. Contributions of features B and C are maximum for methylamine and show a gradual decrease with increasing chain length of the amines. For butylamine, the major contribution is from feature A. In addition, the quadrupolar splitting of B shows a similar trend—maximum for methylamine- and minimum for butylamine-intercalated $FePS_3$. In the assignment of the various components, feature A presents no difficulty. A comparison of the isomer shift and quadrupole splitting with that of $FePS_3$ shows that it corresponds to Fe^{2+} in an $FePS_3$ environment. Feature B has an isomer shift identical to feature A but with a larger quadrupole splitting. The splitting increases from butylamine to methylamine intercalate. This species is tentatively assigned to an Fe^{2+} in a "distorted $FePS_3$"-like environment. The assignment would explain why the isomer shift is identical to that of Fe^{2+} in $FePS_3$ but the quadrupole splitting is larger. The quadrupole splitting (0.6 mm/s) of feature C is identical to that reported for a species observed in the lithium intercalated $FePS_3$ by Colombet et al.[11] The authors say that the Mössbauer spectra of Li_xFePS_3 had been recorded 1 month after intercalation, what they called an "annealing process". On the basis of a comparison of the observed isomer shift with those theoretically calculated by Walker et al.,[24] it had been concluded[10] that on lithium intercalation, Fe^{2+} was reduced to a Fe(0) state. The authors, however, do not comment on the mechanism of the two-electron charge-transfer process. In the case of amine intercalates, however, there are compelling reasons to believe that species C is not a reduced Fe(0) but rather oxidized Fe^{3+}! First, the isomer shifts are comparable to those experimentally observed for a number of Fe^{3+} compounds[25] which are in the range 0.28–0.35 mm/s. Second, when methylamine-intercalated samples were deliberately exposed to the atmosphere so that the samples changed color (as mentioned in the Experimental Section), the Mössbauer spectra show that the only feature observed was C (Figure 4). In fact, the Mössbauer spectra of air-exposed, methylamine-intercalated $FePS_3$ and superparamegnetic Fe_2O_3 are identical. The isomer shift and quadrupole splitting of feature C is identical to those of fine-particle, superparamagnetic Fe_2O_3. The presence of superparamagnetic Fe_2O_3 was further confirmed by magnetic measurements which are discussed in a subsequent section. Consequently feature C, in the Mössbauer spectra of the amine intercalates, is assigned to Fe^{3+}, in an environment similar to that in superparamagnetic Fe_2O_3. The Mössbauer spectra indicate that the materials are biphasic. It was not possible, however, to estimate the relative concentrations from the area under the curves. This would require an exact identification of the phases so that the proper recoilless factor, f, may be chosen. Moreover, even for the intercalated samples of the same amine there were minor variations in the relative contributions of the various features from sample to sample although the positions (isomer shift and quadrupole splitting) remained unchanged. A similar observation had been noticed in the TG and the TPDS.

An important question that arises as a consequence of the above assignment is whether the formation of the Fe^{3+} is due to inadequate precautions during the loading of recording of the Mössbauer spectra or to a product of the intercalation process.

The question may be answered by monitoring the Fe^{3+} concentrations during the intercalation process. EPR spectra would be suitable since the spectra could be recorded in a reasonably short time (5 min). In addition, Fe^{3+} (d^5) is an EPR active ion while Fe^{2+} (d^6), being a Kramers ion, shows no EPR signal.

EPR Spectra. EPR spectroscopy was used to monitor the progress of the intercalation of methylamine in $FePS_3$. The *in situ* experiment was carried out by condensing methylamine on to $FePS_3$ powder in an EPR tube at liquid nitrogen temperature. The tube was sealed and allowed to warm up to room temperature in the EPR spectrometer cavity. Figure 5a shows the EPR spectra at different periods of time after the sample reached room temperature.

The initial spectrum is characteristic of $FePS_3$. As mentioned in the Experimental Section, $FePS_3$ powders give an EPR signal because of Fe^{3+} due to nonstoichiometry. The initial spectra had a line width (peak-to-peak) of 325 G and g = 2.00. During the course of

(24) Walker, L. R.; Wertheim, G. K.; Jaccarino, V. *Phys. Rev. Lett.* 1961, *6*, 98.
(25) *Mössbauer Effect Data Index*; Stevens, J. G., Stevens, V. E., Eds.; IFI/Plenum: New York, 1974.

Table II. Mössbauer Effect Data

compound[a]	quadrupole splitting (mm/s)			isomer shift[b] (mm/s)		
	A	B	C	A	B	C
Fs	1.57 ± .01			0.85 ± .04		
Bu	1.56 ± .02	1.77 ± .08	0.64 ± .04	0.86 ± .04	0.82 ± .06	0.26 ± .06
Pr	1.62 ± .04	1.91 ± .08	0.63 ± .05	0.86 ± .03	0.81 ± .07	0.27 ± .05
Et	1.63 ± .04	2.08 ± .07	0.61 ● .03	0.85 ± .04	0.81 ± .07	0.27 ± .06
Me	1.65 ● .08	2.14 ± .09	0.61 ± .04	0.85 ± .04	0.81 ± .06	0.27 ± .06
Ex			0.62 ± .03			0.28 ± .05

[a] Fs, $FePS_3$; Bu, $FePS_3$–$C_4H_9NH_2$; Pr, $FePS_3$–$C_3H_7NH_2$; Et, $FePS_3$–$C_2H_5NH_2$; Me, $FePS_3$–CH_3NH_2; Ex, air-exposed $FePS_3$–CH_3NH_2. [b] Values with respect to metallic iron.

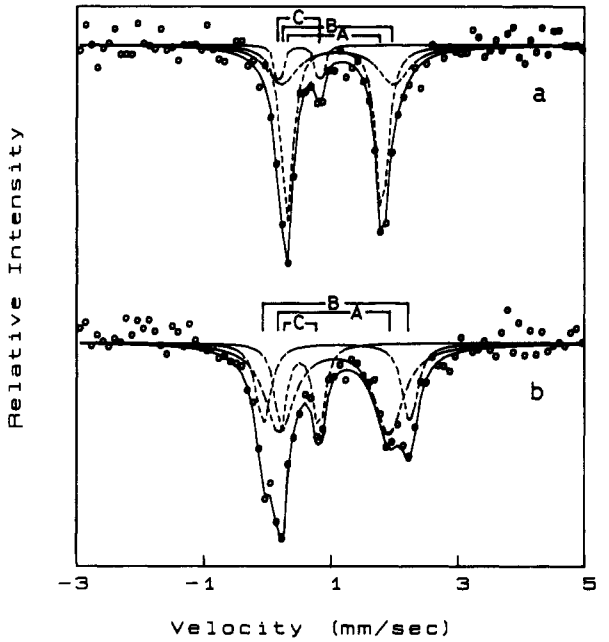

Figure 3. Mössbauer spectra of methylamine- and butylamine-intercalated $FePS_3$. Dotted lines represent individual doublets (marked as A, B, and C), and the solid lines are the sum of the Lorentzians. The circles represent the experimental points: (a) $FePS_3$–$C_4H_9NH_2$; (b) $FePS_3$–CH_3NH_2. Only part of the spectra are shown for clarity.

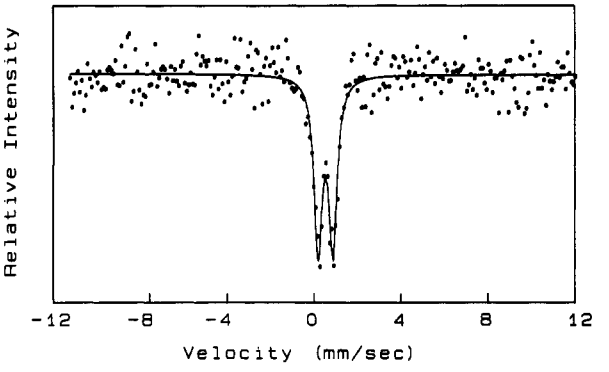

Figure 4. Mössbauer spectrum of air exposed methylamine-intercalated $FePS_3$. Circles are experimental points, and solid line represents the least-squares fitted curve.

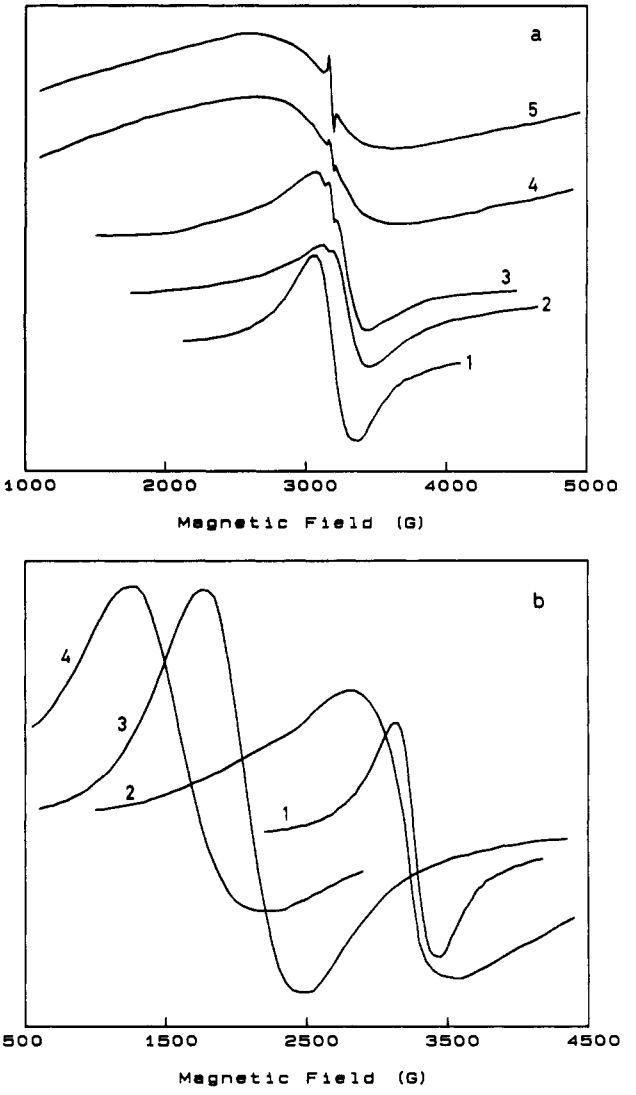

Figure 5. (a) Room-temperature EPR spectra of $FePS_3$, sealed with dry methylamine, at different time intervals: (1) immediately after sealing; (2) after 5 min; (3) after 10 min; (4) after 20 min; (5) after 30 min. (b) Room-temperature EPR spectra of $FePS_3$ and amine-intercalated $FePS_3$ samples: (1) $FePS_3$; (2) $FePS_3$–$C_4H_9NH_2$; (3) $FePS_3$–$C_2H_5NH_2$; (4) $FePS_3$–CH_3NH_2.

intercalation, two additional features appear. The first is what appears as a broadening of the original Fe^{3+} in $FePS_3$ signal. There is a large increase in intensity as well as line width. Both line width (1000 G) and intensity reach a maximum in 30 min, after which there is no change in either parameters but a gradual shift of the resonance to lower fields. The second feature is a sharp resonance at $g = 2.00$. This grows in intensity and then slowly disappears. This feature may be clearly seen in the spectra recorded after 10 min. After 45 min this feature is no longer observed.

The broad feature is assigned to Fe^{3+}. The shift to lower fields is characteristic of magnetic compounds, and takes place because of the internal field. Consequently, the broad peak must be due to Fe^{3+} in superparamagnetic Fe_2O_3 particles.

Since the internal field would be proportional to the size and concentration of Fe_2O_3 (below saturation limit), the above assignment may be easily verified by examining

the EPR spectra of the other amines. Mössbauer spectra had shown that the concentration of Fe^{3+} increases from butyl- to methylamine and that this should be reflected in the observed resonance positions. The EPR spectra of methyl-, ethyl-, and butylamine-intercalated $FePS_3$ are shown in Figure 5b. The spectra were recorded after complete intercalation was verified through XRD. It may be seen that the resonance occurs at lowest fields for methylamine intercalate, for which the concentration of Fe^{3+} is the highest. For butylamine intercalate which has the lowest concentration of Fe^{3+}, the resonance appears at the highest fields. The resonance position for ethylamine intercalate is intermediate between these two values. The above observation confirms that the broad feature is due to Fe^{3+} in a superparamagnetic environment. The EPR spectra confirm that the Fe^{3+} ions are generated during the course of intercalation and not due to later oxidation. It has not been possible to assign the short lived sharp feature at $g = 2.00$. It may be a precursor to the formation of Fe_2O_3.

Although an internal magnetic field has been invoked as the origin of the resonance shifts in the EPR spectra, the Mössbauer spectra does not show the sextuplet splitting expected of a ^{57}Fe nuclei in a field. This apparent difference in the results of the EPR and Mössbauer spectra is because the two techniques probe processes on different time scales. It is well-known[26] that in the measurement of magnetic properties of single-domain particles what is observed depends of the ratio of the time required for the measurement, τ_{obs}, to the relaxation time, τ_0, associated with the change in direction of the magnetization vector of the internal field of the particle. In a Mössbauer experiment, for a ^{57}Fe nuclei τ_{obs} is typically of the order of 2.5×10^{-8} s,[26] whereas in an EPR measurement recorded on an X-band spectrometer τ_{obs} is approximately 1.1×10^{-10} s. Consequently if the relaxation time τ_0 associated with the direction of the magnetization vector of the internal field is between 10^{-8} and 10^{-10} s, the effect of the internal field would not be seen in the Mössbauer spectra but in an EPR experiment. This would probably be realized in Fe_2O_3 particles with diameters ~100 Å. This is likely to correspond to the present situation; the isomer shift and quadrupole splitting of feature C in the Mössbauer spectra (Figure 4, Table II) are similar to that reported by Kündig et al.[26] for Fe_2O_3 particles with average particle size <100 Å.

Magnetic Properties. Detailed magnetic measurements were carried out on powders and crystals of methylamine- and ethylamine-intercalated $FePS_3$. The susceptibility[27] of the crystals along two principal orientation—parallel ($\chi_\perp$) and perpendicular ($\chi_\parallel$) to the layers—as a function of temperature is shown in Figures 6 and 7. The susceptibilities are highly anisotropic ($\chi_\parallel > \chi_\perp$) for both methylamine and ethylamine intercalates, and both compounds exhibit a sharp transition at 78 K. For comparison, the susceptibility of $FePS_3$ is shown in Figure 8. As mentioned in the introduction, the susceptibility of $FePS_3$ is highly anisotropic, $\chi_\parallel > \chi_\perp$. The angular

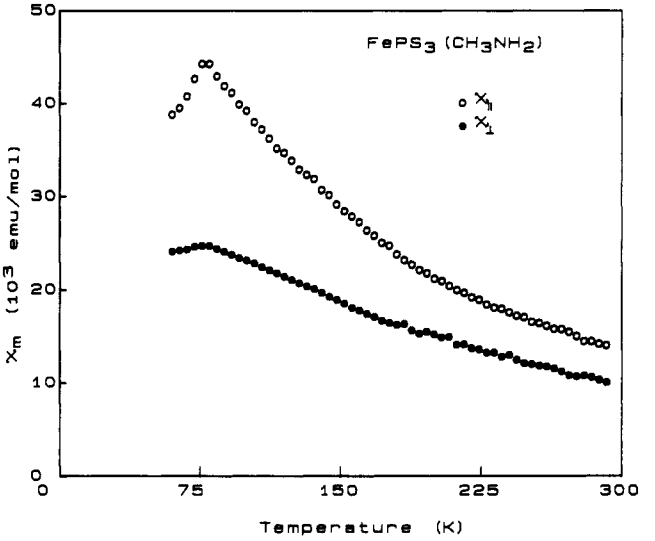

Figure 6. Magnetic susceptibility of methylamine-intercalated $FePS_3$ crystals along two directions as a function of temperature. The superparamagnetic contribution has been subtracted (see text for details).

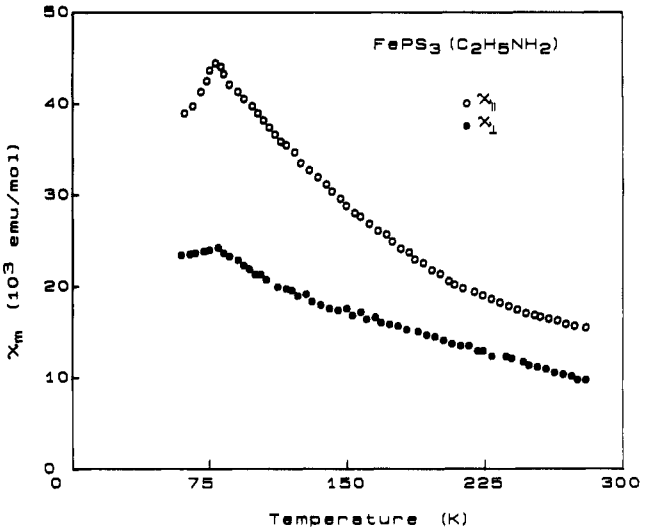

Figure 7. Magnetic susceptibility of ethylamine-intercalated $FePS_3$ crystals along two directions as a function of temperature. The superparamagnetic contribution has been subtracted (see text for details).

dependence of the susceptibility of amine-intercalated $FePS_3$ is similar to that of pure $FePS_3$.

A major difference in the magnetic behavior between amine-intercalated $FePS_3$ and pure $FePS_3$ is the nonlinear M–H behavior of the former. This nonlinear behavior is observed even at high temperatures much above T_c. A typical M–H curve for the intercalated compounds is shown in Figure 9. Such nonlinear M–H behavior with no accompanying hysterisis is characteristic of superparamagnetism. However, a superparamagnetic component alone would not be able to account for all the observed features—anisotropy and the low-temperature transition. This would require a second component, which is paramagnetic, has highly anisotropic susceptibilities, and also undergoes a low temperature transition.

In the light of the previous discussions and the evidence from Mössbauer spectroscopy and EPR, the superparamagnetic component may be identified as fine-particle Fe_2O_3. The presence of the paramagnetic component must be due to a species similar to $FePS_3$, because of the

(26) Kündig, W.; Bömmel, H.; Constabaris, G.; Lindquist, R. H. *Phys. Rev.* **1966**, *142*, 327.

(27) The molar susceptibilities are calculated assuming that the entire weight loss in the TGA is due to deintercalated amine only and the solid residue obtained after deintercalation is pure $FePS_3$. The susceptibilities are then corrected for the presence of ferromagnetic impurities as discussed in a later part of this section.

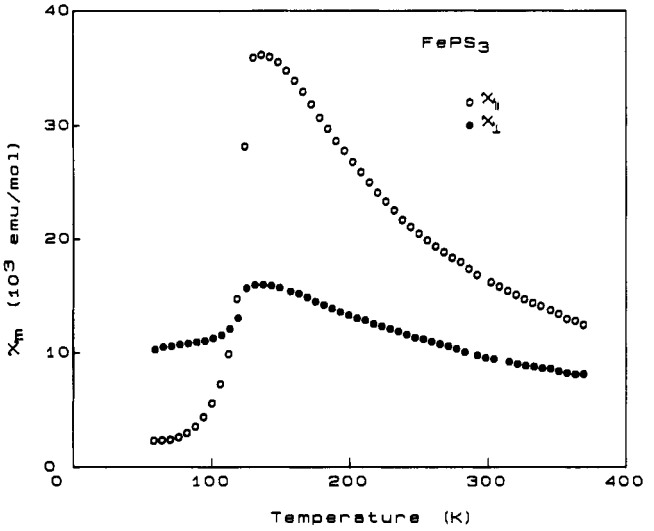

Figure 8. Magnetic susceptibility of $FePS_3$ single crystals parallel ($\chi_\parallel$) and perpendicular ($\chi_\perp$) to the trigonal axis, as a function of temperature.

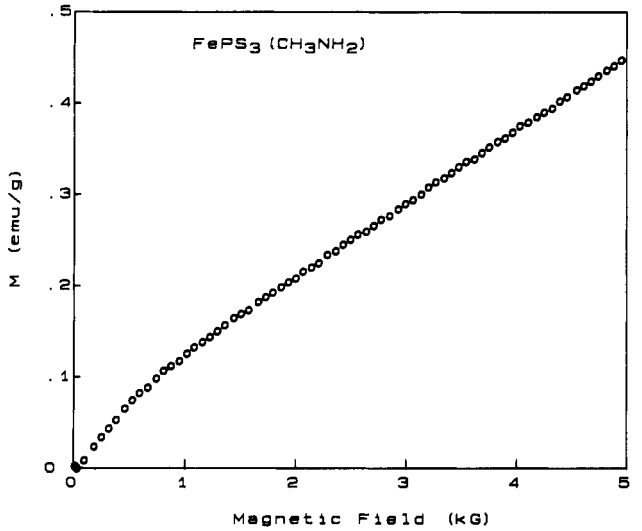

Figure 9. Field dependence of magnetization of methylamine-intercalated $FePS_3$.

similarity in the anisotropy behavior. It is tentatively identified as the $Fe_{1-x}PS_3$(methylamine).

A more detailed analysis of the paramagnetic component would require a method of subtracting the contribution of the superparamagnetic Fe_2O_3 particles. The method of Honda and Owens[28] was adopted. In this procedure the susceptibility is plotted as a function of $1/H$, where H is the applied field. The intercept of the linear plot (high-field limit) on the χ axis gives the true paramagnetic susceptibility, while the slope is proportional to the superparamagnetic contribution. The procedure is strictly valid for ferromagnetic impurities present along with a paramagnetic phase, but can also be used to estimate the contribution of a superparamagnetic impurity phase with the limitation that the concentration of the superparamagnetic phase cannot be calculated since its saturation magnetization is not defined. The contribution of the superparamagnetic component to the overall susceptibility is isotropic. Plots of $\chi_\parallel$ vs $1/H$ and $\chi_\perp$ vs $1/H$ gave identical

(28) The Honda and Owens procedure is taken from: Morris, B. L.; Wold, A. *Rev. Sci. Instrum.* **1968**, *39*, 1938.

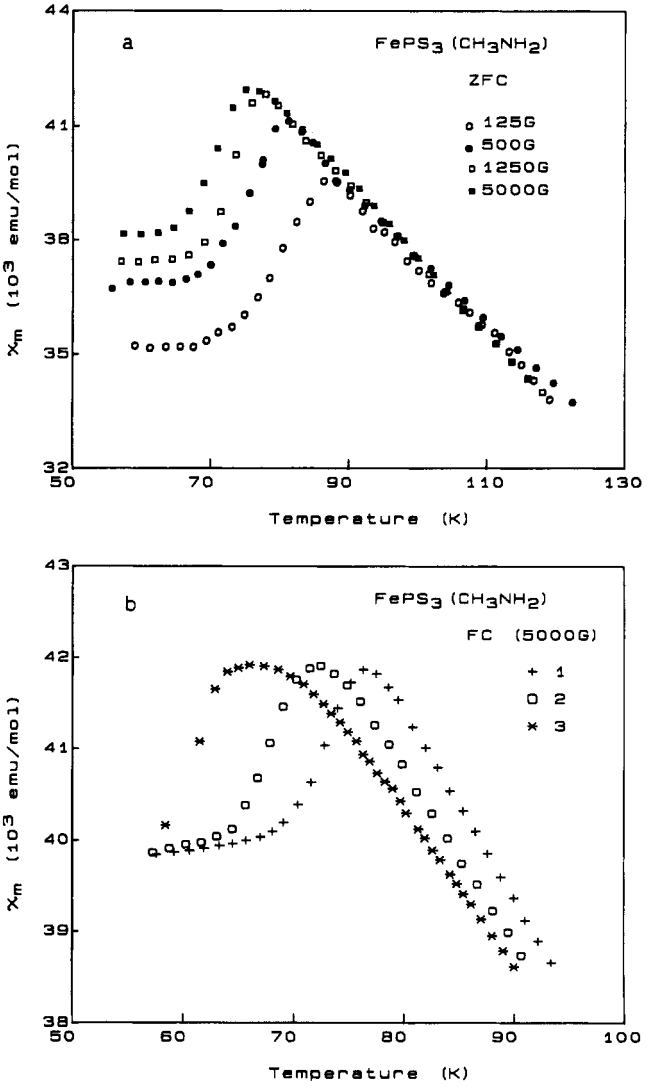

Figure 10. (a) Magnetic susceptibility at different field strengths for methylamine-intercalated $FePS_3$ cooled in zero field (ZFC). (b) Magnetic susceptibility of methylamine-intercalated $FePS_3$ cooled in a field (5000 G) as a function of temperature. 1, 2, and 3 represents consecutive measurements.

values of χ_{sp} (superparamagnetic), although the intercepts were considerably different. The superparamagnetic contribution was found to be temperature independent and consequently could be subtracted from the susceptibility vs temperature plot. The data in Figures 6 and 7 are the corrected values. Since the concentration of the superparamagnetic component could not be estimated, the true paramagnetic susceptibility was also not obtainable, so the true molar susceptibility of the paramagnetic phase could not be calculated.

The most interesting feature in the susceptibility behavior of the amine-intercalated $FePS_3$ is the strong field and history dependence of the transition temperature as well as the sharpness of the transition. For zero-field-cooled (ZFC) samples, the position of the sharp transition (T_c) is pushed to lower and lower temperatures with increasing fields. This is shown in Figure 10a for four different fields. For the same applied field, samples cooled in the field (FC) showed a shift in the transition temperature to lower values. Repeated cycling (warming and cooling of the sample in a magnetic field) appears to destroy the transition completely. This behavior is shown in Figure 10b for three consecutive cycles. It may be pointed out

that this behavior is quite different from that expected of a spin glass.[29]

In the Introduction it had been mentioned that the Ising nature of magnetic interactions in $FePS_3$ arises from the anisotropy in the expectation value of the spin moments due to the large single ion anisotropy. Since the high-temperature susceptibility and anisotropy of the amine-intercalated $FePS_3$ are comparable to those of pure $FePS_3$, it appears that the Ising nature of magnetic interactions are preserved even after intercalation. However, the low temperature susceptibility behavior—the sharp transition at temperatures lower than T_N and the field dependence of T_c—suggests a new phenomenon which is entirely different from that in pure $FePS_3$.

Amine Intercalation in $FePS_3$: The Mechanism. Any mechanism proposed for the intercalation of amines in $FePS_3$ would have to account for the experimental observations of the preceding sections, which are summarized here:

(i) There appears to be more than one "type" of intercalated amine species, and their relative concentrations depend on the extent of drying of the amine prior to intercalation as well as exposure of the intercalated samples to the atmosphere. The presence of water in the amine appears to play a crucial role. There is indirect evidence that the intercalated species are the protonated cation (RNH_3^+) and neutral amine (RNH_2).

(ii) No Fe^{2+} is detected in the supernatant amine solution after intercalation, and there was no sulfur dissolution in the amine during the course of the intercalation.

(iii) The amine-intercalated $FePS_3$ is much more susceptible to oxidation than pure $FePS_3$, i.e., oxidation leading to the formation of Fe_2O_3.

(iv) There is practically no change in the electrical conductivity of $FePS_3$ on intercalation, suggesting either that there is no charge transfer from amine to the host or that charge is transferred to localized electronic states of the host lattice.

(v) Mössbauer spectra of the amine-intercalated compounds show that some, but not all, Fe^{2+} sites are distorted from the $FePS_3$ geometry.

(vi) Mössbauer spectra show no evidence for a reduced species (oxidation state less than 2+) but indicate the presence of an oxidized, Fe^{3+} species. The presence of superparamagnetic Fe^{3+}, probably Fe_2O_3, was confirmed by EPR spectra and magnetic susceptibility measurements. Fe^{3+} is formed during the intercalation process.

The mechanism proposed is similar to that for pyridine intercalation in $MnPS_3$.[13] The intercalated species are the charged alkylammonium cations solvated by neutral amine and/or H_2O molecules. Charge neutrality is maintained by the removal of an appropriate number of Fe^{2+} ions from the lattice. The Fe^{2+} ions removed from the lattice are further oxidized by H_2O/O_2 to Fe^{3+} species.

The overall reaction scheme is as follows: the first step is the formation of the alkylammonium cations similar to that proposed by Schöllhorn[30] for the intercalation in the transition-metal dichalcogenides:

$$RNH_2 + H_2O \rightleftharpoons RNH_3^+ + OH^-$$

Thermal deintercalation spectra provide indirect evidence that one of the intercalated species is the alkylammonium cation, the other species being neutral amine and/or H_2O molecules. The second step is the ion exchange/intercalation reaction:

$$FePS_3 + 2xRNH_3^+ + yRNH_2 \rightarrow Fe_{1-x}PS_3(RNH_3^+)_{2x}(RNH_2)_y + xFe^{2+}$$

The Fe^{2+} ions removed from the lattice are subsequently converted to Fe_2O_3:

$$2Fe^{2+} + 6OH^- \xrightarrow[\text{oxd(?)}\quad\text{red(?)}]{} Fe_2^{3+}O_3^{2-} + 3H_2O$$

It may be seen that in the above scheme, although mass balance is satisfied, charge balance is not, unless the reaction is coupled to another redox pair. The complementary reduced species have not been identified, but it is unlikely to be a lattice site, since that would not be in keeping with observations v and vi. The reduced species is likely to be trace amounts of water present in the amine. The sharp short-lived EPR signal (Figure 5a) may be an evidence for such a reaction. As long as the Fe^{2+}–Fe^{3+}/oxd–red coupled reaction takes place outside the $FePS_3$ lattice without involving any lattice species, the identification of the complementary redox pair is not crucial to the understanding of the properties of the amine-intercalated $FePS_3$. The crucial step is really the formation of Fe^{2+} vacancies by which charge neutrality is maintained. The fate of the removed Fe^{2+} ions does not have any bearing on the mechanism of intercalation.

The above reaction schemes would be able to account for observations i–vi.

There are at least two types of amines—the protonated alkylammonium cation and neutral amines which solvate it. The source of protons is H_2O molecules. The neutral amines may undergo exchange with neutral water molecules. The thermal deintercalation has to proceed by a breaking up of the lattice.

Electrical conductivity does not change since there is no charge transfer, charge neutrality being maintained by removal of Fe^{2+} ions to give $Fe_{1-x}PS_3$. In the $Fe_{1-x}PS_3$ lattice, those FeS_6 polyhedra neighboring a vacancy would be distorted whereas those further away from the vacancy would show little change from the $FePS_3$ geometry. The distorted FeS_6 polyhedra should have a ^{57}Fe isomer shift similar to the undistorted FeS_6 polyhedra but a larger quadrupole splitting. Thus the presence of features A and B in the Mössbauer spectra may be accounted for.

The Fe^{3+} species, as mentioned earlier, is formed by the subsequent oxidation of the Fe^{2+} ions removed from the $FePS_3$ lattice.

On exposure of the amine intercalates to air, there could be further protonation of the amine by atmospheric water. This would require further removal of Fe^{2+} ions from the lattice which would be subsequently oxidized to Fe_2O_3. Unlike sealed-tube conditions, there is no concentration limitation of H_2O or O_2 so that the reaction can proceed to complete conversion of Fe^{2+} to Fe_2O_3.

Finally we shall examine how far an $Fe_{1-x}PS_3$ lattice would explain the field and temperature dependence of the observed magnetic susceptibility. As mentioned, the Ising nature of the magnetic interactions is preserved so that the system would now correspond to a 2D antiferromagnetic Ising lattice with random defects. The problem

(29) Binder, K.; Young, A. P. *Rev. Mod. Phys.* **1986**, *58*, 801.
(30) Lerf, A.; Schöllhorn, R. *Inorg. Chem.* **1977**, *16*, 2950.

of antiferromagnetic Ising lattices with defects has been studied by various groups[31] and has been discussed as the random field Ising model (RFIM). It was first shown by Fishman and Aharony[32] that a dilute Ising antiferromagnet in the presence of an external field, H, parallel to the easy axis constitutes a physically realizable RFIM. A dilute antiferromagnet exhibiting random field magnetic behavior is expected to show a sharp transition at $H = 0$. With increasing field strength, a gradual decrease in T_c with a rounding of the transition is expected due to the destruction of the long-range ordered (LRO) states. There are numerous examples, of both 3D ($Fe_{0.68}Zn_{0.32}F_2$, $Mn_{0.75}Zn_{0.25}F_2$, etc.) as well as 2D ($Rb_2Co_{0.85}Mg_{0.15}F_4$) materials, where many of the expected features of the RFIM have been observed.[33]

The experimental situation is however confused by the history dependence of many of the observed features which obscure the theoretically anticipated changes.[34] The origin of this is domain formation. The LRO states which should have been destroyed by the external field create domains. These domains are difficult to destroy since the nonmagnetic impurities or diluents, which are necessary to generate the random field constitute natural pinning centers for the domain walls; interfaces may thereby become frozen in hardy, long-lived metastable configurations, which manifest experimentally as history-dependent behavior or long equilibrium times.[35]

The amine-intercalated $FePS_3$ shows many of the features attributed to an RFIM—a sharp transition which shifts to lower temperatures with increasing field strengths. However, no rounding of the transition, comparable to the other 2D systems is observed even at the highest field strengths. The FC susceptibility shows a transition at a lower temperature than that of ZFC, but with comparable sharpness. Repeated cycling through the transition temperature in the presence of a field, however, appears to destroy the LRO state. This may be seen in Figure 9b, where, rounding of the peak with a gradual decrease in T_c on cycling is observed. The transition in the ZFC as well as the initial FC sample may thus be considered as arising from LRO states locked in metastable domains. These domains show considerable stability and are not easily destroyed because of the pinning of the domain walls by the defect, cation vacancies. On repeated cycling through T_c, however, there is an increasing probability of unpinning of the domain walls leading to the destruction of the LRO states. The formation of such a domain explains why the initial FC susceptibility shows a transition lower in temperature than that of ZFC, but with the same sharpness. Such history dependent effects due to domain formation have been previously observed in $Fe_{1-x}Zn_xF_2$, in neutron scattering experiments.[36]

The observed susceptibility behavior is in qualitative agreement with many of the features expected of an RFIM. There is no doubt that a diluted Ising system, $Fe_{1-x}PS_3$, is at work. But whether the system truly conforms to an RFIM can be viewed only through further experiments. In the $Fe_{1-x}PS_3$ lattice, the random effects could arise either from vacancies or from the Fe^{2+} ions neighboring a vacancy, which are distorted from the $FePS_3$ geometry (feature B, Mössbauer spectra) and may have a different single-ion anisotropy from the rest of the Fe^{2+} ions (feature A, Mössbauer spectra).

Thus, the magnetic susceptibility confirms the presence of both a superparamagnetic Fe_2O_3 and an $Fe_{1-x}PS_3$ species, and the suggested mechansim appears to be justified.

Acknowledgment. The authors acknowledge the help of K. R. Kannan in recording the Mössbauer spectra and to Dr. Thomas Chacko for a critical reading of the manuscript. P.A.J. is grateful to CSIR, INDIA for a research fellowship.

(31) Shapira, Y. *J. Appl. Phys.* **1985**, *57*, 1938. Imry, Y. *J. Stat. Phys.* **1984**, *34*, 849. Pyite, E.; Fernandez, J. F. *J. Appl. Phys.* **1985**, *57*, 3274. Birgenean, R. J.; Cowley, R. A.; Shirane, G.; Yozhizawa, H. *J. Stat. Phys.* **1984**, *34*, 817. Belanger, D. P.; Young, A. P. *J. Magn. Magn. Mater.* **1991**, *100*, 272.

(32) Fishman, S.; Aharony, A. *J. Phys.* **1979**, *C12*, 1729.

(33) Belanger, D. P.; King, A. R.; Jaccarino, V. *J. Appl. Phys.* **1984**, *55*, 2383. Belanger, D. P.; King, A. R.; Jaccarino, V.; Cardy, J. L. *Phys. Rev.* **1983**, *B28*, 2522. Ferreira, I. B.; King, A. R.; Jaccarino, V.; Cardy, J. L. *Phys. Rev.* **1983**, *B28*, 5192.

(34) Shapira, Y. *Phys. Rev.* **1987**, *B35*, 62.

(35) Grinstein, G. *J. Appl. Phys.* **1984**, *55*, 2371.

(36) Hagen, M.; Cowley, R. A.; Satija, S. K.; Yoshizawa, H.; Shirane, G.; Birgeneau, R. J.; Guggenheim, J. *Phys. Rev.* **1983**, *B28*, 2602.